Size and temperature effects on the thermoelectric power and electrical resistivity of bismuth telluride thin films

V. Damodara Das and N. Soundararajan
Thin Film Laboratory, Department of Physics, Indian Institute of Technology, Madras 600 036, Tamilnadu, India
(Received 7 May 1987; revised manuscript received 22 October 1987)

Thermoelectric power and electrical resistivity measurements have been carried out as a function of temperature in the range 300–470 K on well-annealed thin films of Bi_2Te_3 of various thicknesses in the range 400–1900 Å. The films of a given thickness for both the measurements have been prepared simultaneously in a single evaporation so that the results of the thermoelectric power and the electrical resistivity measurements can be combined to evaluate useful material parameters. Annealed Bi_2Te_3 thin films of all thicknesses exhibit semiconducting behavior, viz., an exponential decrease of resistivity with increasing temperature and a mildly temperature-dependent thermoelectric power, the latter's magnitude increasing with increasing temperature. (The thermoelectric power of all the Bi_2Te_3 thin films is negative, indicating that the majority of carriers are electrons.) The effective-mean-free-path model and least-squares fitting by local (spline) functions have been used to analyze the thickness dependence of thermoelectric power and electrical resistivity of Bi_2Te_3 thin films. Both are found to be linear functions of inverse thickness. By combining the results of analyses of electrical resistivity data and thermoelectric power data, material parameters like mean free path, carrier concentration, their effective mass, and Fermi energy have been evaluated.

INTRODUCTION

Bismuth telluride is a compound semiconductor of narrow band gap of 0.2 eV. Its promise as a good material for thermoelectric applications has stimulated interest in its basic properties. It is an amphoteric semiconductor. Though tellurium deficiency leads to *p*-type conduction and an excess gives rise to *n*-type materials, chemical and x-ray analyses show no difference in composition between *p*-type and *n*-type bismuth telluride.

Bismuth telluride belongs to the crystal class $R\bar{3}m$ and therefore possesses the associated anisotropy of transport parameters. The atoms in bismuth telluride structure are arranged in layers which are stacked in the rhombohedral $\langle 111 \rangle$ direction. The high ratio of the electrical conductivity to the thermal conductivity makes bismuth telluride a good thermoelectric material. Properties such as the resistivity, the Hall constant, etc., vary appreciably with the composition, defects, and texture. Changes in the semiconducting properties of the Bi-Te system with nonstoichiometry are most pronounced in the compound having a stoichiometric composition Bi_2Te_3. Stoichiometric Bi_2Te_3 dissolves about 1% tellurium and does not dissolve bismuth at all.

Even though a significant amount of work has been done on Bi_2Te_3 in the bulk state,[1–7] a very limited amount of work has been carried out on it in the thin-film state.[8–11] In the present study, thermoelectric and electrical conductivity studies have been carried out on thin films of various thicknesses; films of each thickness for both the studies were prepared simultaneously.

EXPERIMENT

A stoichiometric mixture of pure bismuth and tellurium (2:3 atomic ratio) was melted in an evacuated quartz ampoule to prepare a high-purity bismuth telluride bulk alloy. The alloy formation and its homogeneity were confirmed by x-ray powder photography.

To prepare bismuth telluride films, the Bi_2Te_3 alloy was evaporated at a pressure of about 3×10^{-5} torr in a conventional vacuum system. The films with thicknesses varying from 400 to 1 900 Å, were deposited onto well-cleaned glass substrates held at ~300 K during deposition and kept at a distance 30 cm away from the source of evaporation, vertically above it. The glass substrates were cleaned with warm fresh chromic acid, distilled water, and isopropyl alcohol, in that order, before using them for thin-film deposition. The films were deposited at a constant rate of 10 Å/sec. The thicknesses of the films were monitored using a quartz-crystal thickness monitor. The film dimensions were $3\times1\times t$ cm for the resistance measurements and $6.5\times0.5\times t$ cm for the Seebeck coefficient measurements, where t is the thickness of the film. Tin contact films were used for conductivity measurements since silver and copper films were found to react with the bismuth telluride films at the areas of contact. The films of a given thickness for the Seebeck coefficient and resistivity measurements were prepared in a single evaporation using suitable masks. In each evaporation, a given quantity of the bulk alloy was taken in the boat and was completely evaporated at a fast rate (10 Å/sec) to avoid fractionation and to maintain the same average composition in the thin films as that of the bulk alloy.

All the measurements were made on well-annealed films because the preliminary measurements made on as-grown thin films both during heating and cooling cycles showed that the variations of thermoelectric power and electrical resistivity with temperature were different during heating and cooling. During the second cycle of heat-

ing and cooling the temperature dependence in the first cycle-cooling curve was nearly reproduced. Films for these preliminary measurements were prepared simultaneously with the final experimental films which were subsequently annealed at about 470 K for one hour in high vacuum to eliminate most of the irreproducible behavior. To anneal the films, they were slowly heated to above 470 K at a pressure of 2×10^{-5} torr and kept at that temperature for about an hour. After annealing, the films were allowed to cool down to room temperature in vacuum.

The integral method was used to determine the Seebeck coefficient. As the temperature of the hot end varied from 300 to 500 K, the temperature of the cold end was maintained at a constant temperature of 300 K (room temperature). The Seebeck coefficient, i.e., the derivative of the thermal emf with respect to temperature was calculated at different temperatures. Potentiometers and sensitive null detectors (10^{-9} A/div) were used to measure the temperature and the thermal emf. The thermal emf was measured to an accuracy of a microvolt. A Wheatstone network was used to measure the resistance to an accuracy of 1 Ω. Both the thermal emf and electrical resistance measurements were made in the temperature range between 300 and 470 K at intervals of 2 K in a vacuum of 2×10^{-5} torr.

RESULTS

Figures 1 and 2 illustrate that the temperature behaviors of the thermoelectric power and the electrical resis-

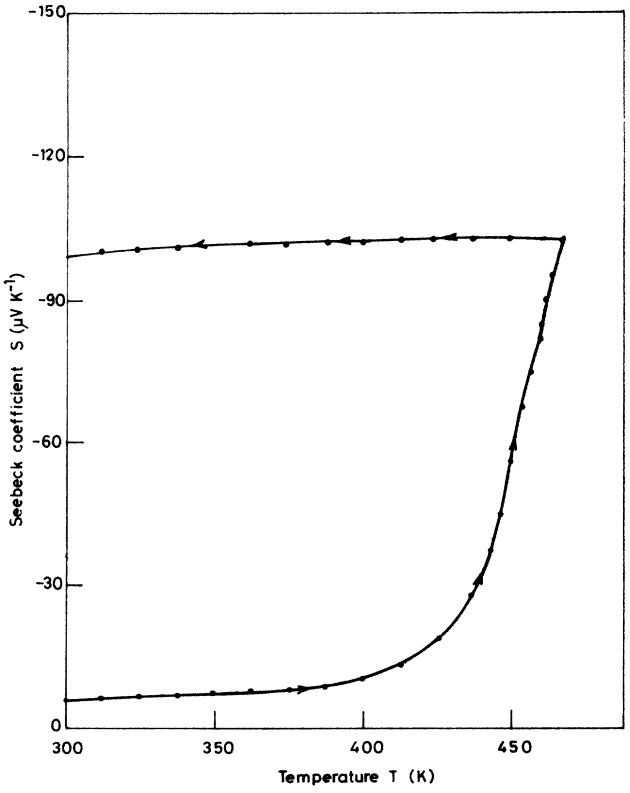

FIG. 1. The variation of Seebeck coefficient as a function of temperature for unannealed film of thickness 690 Å during heating and cooling cycles.

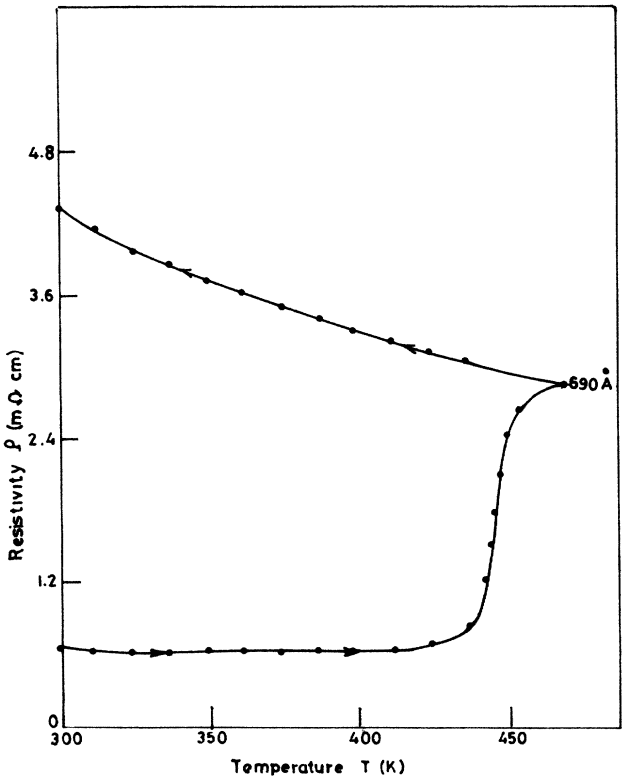

FIG. 2. The variation of resistivity as a function of temperature of unannealed film of thickness 690 Å during heating and cooling cycles.

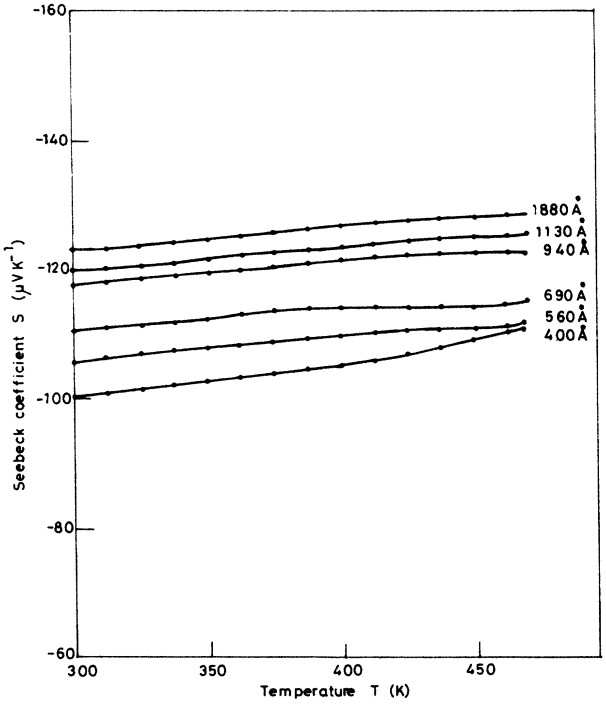

FIG. 3. The variation of Seebeck coefficient as a function of temperature for films of different thicknesses.

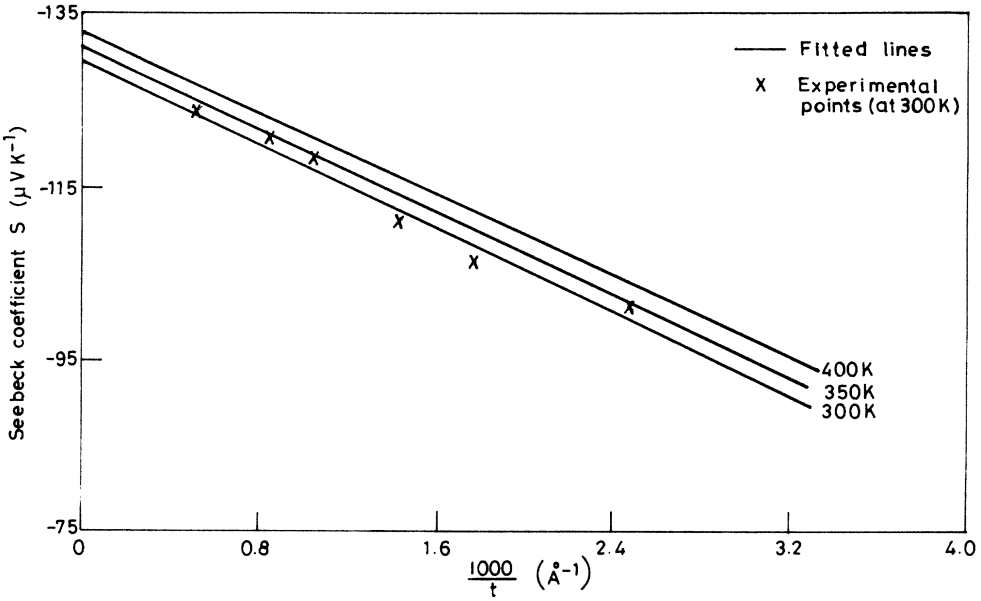

FIG. 4. The thickness dependence of Seebeck coefficient at different temperatures (300, 350, and 400 K).

tivity of as-grown (unannealed) thin films are different during heating and cooling cycles. Therefore, to analyze the temperature and size-effect behavior of thermoelectric power and electrical resistivity, only the data of the well-annealed Bi_2Te_3 films were used. We emphasize that during the second cycle of heating and cooling, the variations follow nearly the variation in the first-cycle cooling.

Figure 3 shows the temperature dependence of the thermoelectric power with temperature of well-annealed (at 470 K for 1 h) Bi_2Te_3 thin films of different thicknesses. It is seen from the figure that the magnitude of thermoelectric power is high for all the thicknesses and increases slowly and nearly linearly with increase in temperature in all cases; this is similar to the behavior during the cooling cycle of the unannealed films (after heating) (cf. Fig. 1). However, it should also be pointed out that the magnitude of the thermoelectric power value of well-annealed films (Fig. 3) is slightly higher than that of unannealed films during the cooling cycle (i.e., after heating to about 470 K) [e.g., compare the thermoelectric powers of the 690-Å film in Fig. 1 during cooling with that of the same thickness (but a different) film in Fig. 3]. This difference can be attributed to two facts. Firstly, the heat cycled film (in Fig. 1) was at a temperature of 470 K for a maximum of 5 min only while the well-annealed films (in Fig. 3) were at the temperature of 470 K for 1 h. Secondly, the film of Fig. 1 was only heated at one end (the hot end) for the thermoelectric power measurement during heating, and hence the temperature of only a part of the film reached 470 K while the temperature of the other parts varied between 470 K and room temperature ($\sim$300 K). As the thermoelectric power increases (in magnitude) on heating, this additional increase in the magnitude of thermoelectric power of well-annealed films is understandable and is due to the two reasons given above.

To analyze the thickness dependence of thermoelectric power, plots of thermoelectric power against the reciprocal of thickness at different temperatures were drawn. The plots at all the three temperatures (300, 350, and 400 K) were linear. Figure 4 shows the least-squares-fitted straight-line plots of thermoelectric power against re-

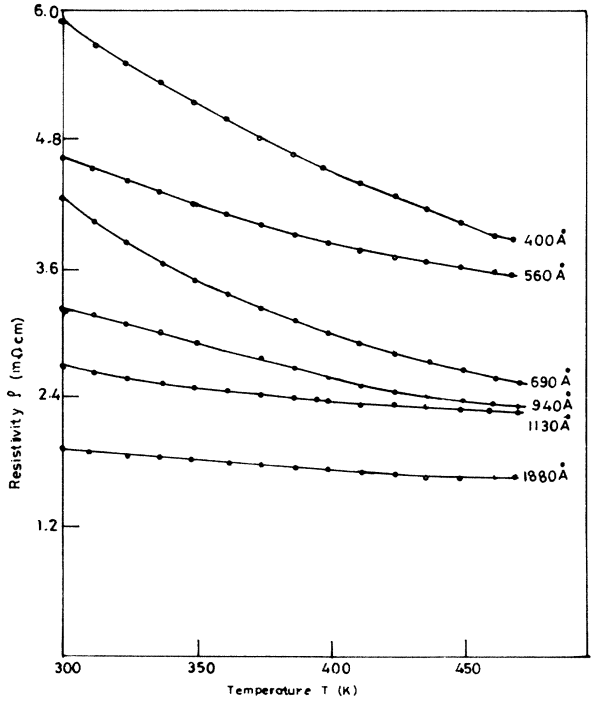

FIG. 5. The variation of resistivity as a function of temperature for films of different thicknesses.

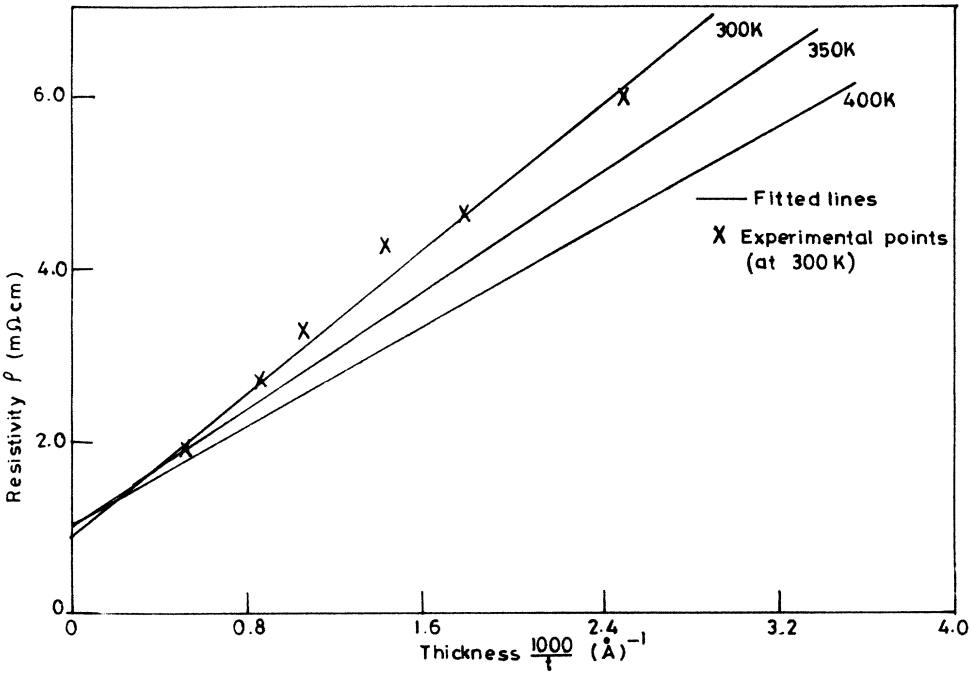

FIG. 6. The thickness dependence of resistivity at different temperatures (300, 350, and 400 K).

ciprocal thickness at different temperatures. Also shown in the figure are experimental points at 300 K.

The resistivity has been plotted as a function of temperature in Fig. 5 for annealed films of different thicknesses. Figure 6 gives the least-squares-fitted plots of the resistivity of annealed bismuth telluride films at three different temperatures (300, 350, and 400 K) as a function of the reciprocal of thickness. Experimental points at 300 K are also shown in the figure. The resistivity also shows a linear dependence on inverse thickness at all three temperatures.

DISCUSSION

In spite of detailed studies on the bulk compound, very few systematic studies have been carried out on thin films as mentioned earlier. The present study is an attempt to understand the electrical properties of bismuth telluride in the thin-film state.

It is seen from Figs. 1 and 2 that thermoelectric power and resistivity of the as-grown (unannealed) films behave radically differently from those after heating. During the subsequent heating and cooling cycles, temperature dependence of the thermoelectric power and resistivity were similar to the temperature dependence during the first cooling. Thus, the behavior of the unannealed films changes irreversibly during the heating.

A. Temperature dependence of Seebeck coefficient and resistivity

As seen from Figs. 3–6, Seebeck coefficient and electrical resistivity of the annealed films are temperature and thickness dependent. The temperature dependence of the Seebeck coefficient of bismuth telluride films shown in Fig. 3 can be explained as follows. Bismuth telluride is an n-type semiconductor. The Seebeck coefficient of an n-type semiconductor is given by[12]

$$S_F=\frac{k}{e}\left[\frac{5}{2}+p-\frac{E_c-E_F}{kT}\right],$$

where E_c is the bottom of the conduction band, E_F the Fermi energy, and T the absolute temperature. e is the electronic charge and k the Boltzmann constant. p is the exponent of the power function in the energy-dependent relaxation time expression. E_C-E_F is nearly constant as T varies. The Seebeck coefficient is weakly temperature dependent, the magnitude increasing with temperature. Goldsmid[13] observed that the Seebeck coefficient is temperature dependent in the range 77 to 300 K. Goswami and Koli[8] measured the Seebeck coefficient of thin films above 300 K and observed a weak temperature dependence, similar to our present observations. Mansfield and William[14] found that the temperature dependence of the Seebeck coefficient depended on the carrier concentration and degeneracy.

Drabble *et al.*[15] measured the resistivity of bismuth telluride in the interval 77 to 300 K. They found that the carriers were strongly degenerate, and hence the resistivity increased with rising temperature. However, Goldsmid[16] observed the semiconducting behavior of resistivity, which decreased with increasing temperature. He also found that if bismuth telluride was properly doped with halogens, the carrier concentration could be varied from degenerate to nondegenerate. In the case of one specimen, he was able to determine the band gap of the material as 0.16 eV. Mansfield and William[14] measured the resistivity as a function of temperature. They

found that initially the resistance increased with temperature at low temperatures, but then decreased with a further increase in temperature. They discussed their results, considering that extrinsic and intrinsic conductions were comparable. In the present studies, all the films exhibit semiconducting behavior in the range of temperatures studied as seen from Fig. 5.

To examine the temperature dependence of the resistivity in more detail, $\ln\rho$ versus $1/T$ plots were drawn as shown in Fig. 7. It is clear from Fig. 7 that the plots are linear for all the films. Thus, Bi_2Te_3 thin films studied in the present work exhibit the normal semiconducting behavior of exponential decrease of resistivity with temperature. The activation energies calculated from the above plots for the films of different thicknesses are tabulated in Table I. They are in the range 12 to 35 meV but do not depend on thickness systematically. However, it is seen from Fig. 7 and the table that there is a tendency for the activation energy to increase as the thickness decreases. Goswami and Koli[8] measured the resistivity of films as a function of temperature and found that the resistivity decreased with increasing temperature. Goswami and Koli observed that $\ln\rho$ versus $1/T$ plots showed two slopes. We find, however, that we get a good linear fit in the entire region studied.

The discrepancies between the temperature dependence of the thermoelectric power and resistivity (especially the latter) observed by earlier workers is most probably due to their measurements being made on the unannealed films and to their preparation under different conditions, leading to thin films of different compositions (stoichiometries) and different irreversible changes upon heating. Our work shows that reproducible behavior of Bi_2Te_3 thin films can be obtained only after careful annealing of the films to remove irreversible changes on heating.

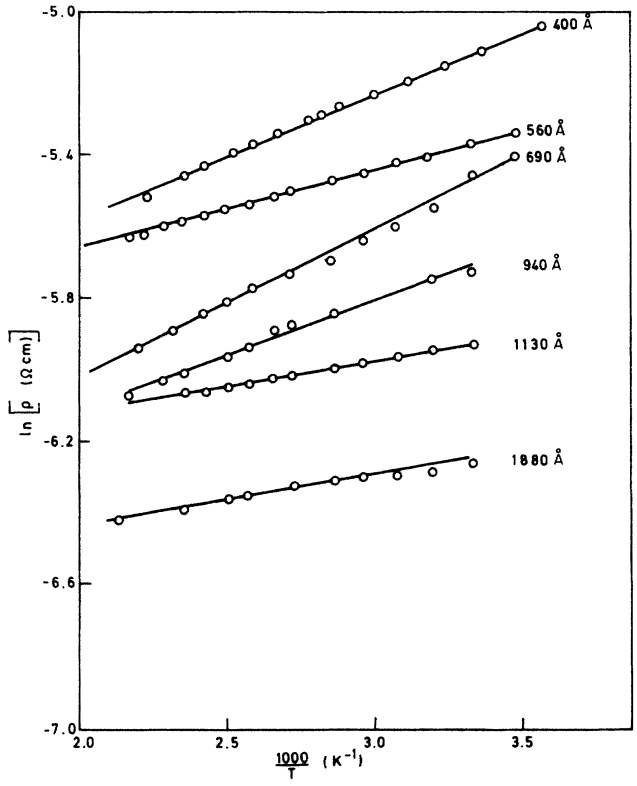

FIG. 7. The variation of logarithmic resistivity as a function of the reciprocal of temperature for films of different thicknesses.

TABLE I. The activation energies calculated from $\ln\rho_f$ vs $1/T$ plots of films of different thicknesses.

Serial number	Thickness (Å)	Activation energy (m eV)
1	400	29.3
2	560	17.2
3	690	35.3
4	940	26.0
5	1130	12.1
6	1880	12.7

B. Thickness dependence of Seebeck coefficient and electrical resistivity

In thin films, the surface and grain-boundary scatterings should be taken into account along with the defect scattering and phonon scattering, when its transport properties are discussed. Sondheimer[17] in his discussion on the thickness dependence of resistivity, considered surface scattering with the other normal bulk scattering. He obtained the expression,

$$\rho_f=\rho_0\left[1-\frac{3(1-p)}{2K_0}\int_1^\infty\left(\frac{1}{x^3}-\frac{1}{x^5}\right)\times\frac{1-\exp(-K_0x)}{1-p\exp(-K_0x)}dx\right]^{-1},$$

where ρ_f and ρ_0 are the film resistivity and bulk resistivity, $K_0=t/l_0$ where t is the thickness of the film and l_0 is the bulk mean free path. p is called the specularity parameter which gives the fraction of carriers which are specularly scattered from the surfaces. x is the integration variable related to the angle of incidence of the charge carriers at the surface θ, and is given by $x=1/\cos\theta$. The specularly scattered carriers do not contribute to size effects in resistivity (and thermoelectric power) of thin films as they are scattered without loss of motion parallel to the surfaces. In the present study, we assume $p=0$ so that all the carriers are diffusely scattered from the surfaces and hence contribute to size effects. Thus, a maximum amount of size effect is taken to be present (and effective).

The analysis of the experimental observations using this expression leads to the evaluation of bulk resistivity and mean free path of the carriers. But the estimated parameters will be erroneous. This is because, in films, the average size of the crystallites is proportional to film thickness (a few hundred Å) and hence grain-boundary scattering becomes important in determining transport properties.

Mayadas and Shatzkes,[18] taking into account the

grain-boundary scattering, modified the Fuch-Sondheimer theory, but the expression in their theory is complicated; therefore, a few attempts[19–21] have been made to simplify the expression.

Tellier[21] succeeded in deriving a simplified analytical expression for the electrical resistivity of films as a function of thickness. In her analysis, she postulated a hypothetical bulk having the same film texture and microstructure. This hypothetical bulk is nothing but the film of infinite thickness. Because this bulk has the same microstructure (grain size and grain boundaries) as that of the (polycrystalline) films, the mean free path of carriers in the (ideal) bulk, l_0, will be different from that of the infinite thick film (hypothetical bulk), l_g. The infinite film resistivity ρ_g will be higher than the bulk resistivity ρ_0. According to the effective-mean-free-path model, the analytical expression for the film resistivity is

$$\rho_f=\rho_g\left[1-\frac{3(1-p)}{2K_g}\int_1^\infty\left(\frac{1}{x^3}-\frac{1}{x^5}\right)\times\frac{1-\exp(-K_g x)}{1-p\exp(-K_g x)}dx\right]^{-1}$$

In this equation also, the symbols ρ_f, p, and x have the same meaning as before. The ratio $K_0=t/l_0$ is replaced by the ratio $K_g=t/l_g$ where l_g is the mean free path in the infinite thick film (or the hypothetical bulk); ρ_g is its resistivity. The above expression is identical to that of Fuch-Sondheimer's theory with the replacement of ρ_g for ρ_0 and l_g for l_0.

The asymptotic expression when $K_g>1$ is $\rho_f=\rho_0[1+\frac{3}{8}(1-p)/K_g]$. This equation is found to explain satisfactorily the variation of resistivity with thickness of films of thicknesses greater than $0.1l_g$. Thus, the experimental data on resistivity should exhibit a reciprocal thickness dependence as $K_g=t/l_g$, where t is the thickness. It is evident from Fig. 6 that indeed resistivity of Bi_2Te_3 thin films varies linearly with the reciprocal of thickness not only at room temperature (300 K) but also at 350 and 400 K.

At 300, 350, and 400 K, the resistivities of the infinite thick film are 0.98, 1.0, 1.0 mΩ cm. Ainsworth[22] found that the ingots prepared by him had a resistivity about 2 mΩ cm. Drabble *et al.*[15] measured the resistivity of single crystals as 1.2 mΩ cm. Goldsmid[13] prepared bulk materials of resistivity varying from 0.2 to 1 mΩ cm. The mean free paths determined by us at 300, 350, and 400 K are 5540, 4360, and 3680 Å. These values are less than the values obtained by Goswami and Koli,[32] viz., 5960 and 5540 Å at 300 and 350 K.

Mayer[23] was the first to analyze the thickness dependence of the Seebeck coefficient of thin films. He took into account only the surface scattering, in addition to bulk scattering. A few more theories[24–26] have analyzed the thickness dependence of the Seebeck coefficient, but the effective-mean-free-path model developed by Pichard *et al.*,[26] taking into account the grain-boundary scattering, is the simplest basis for discussion.

According to this model, the Seebeck coefficient of a thin film S_f is given by

$$S_f=S_g\left[1-\frac{3}{8}\frac{(1-p)l_g}{t}\frac{U}{1+U}\right],$$

where S_g is the Seebeck coefficient and l_g is the mean free path of carriers in the infinite thick film. U is the exponent of the energy term in the energy-dependent mean free path, t the film thickness, and p the specularity parameter. It is clear from the above expression that the thermoelectric power should also depend linearly on the reciprocal thickness of the thin films. It is evident from the plots of Fig. 4 that the thin-film thermoelectric power is linearly dependent on the inverse thickness of the films at all three constant temperatures (300, 350, and 400 K).

If the microstructure of the films used for thermoelectric power measurements and electrical resistivity measurements is the same, the mean free path for conduction will be the same in the two sets of films. Then, it is possible to combine the results obtained from the analysis of both the resistivity data and thermoelectric power data and obtain useful material parameters like Fermi energy, electron concentration, and electron effective mass. As in the present study, films for both thermoelectric power and electrical resistivity measurements were prepared simultaneously in a single evaporation, and each evaporation was similar to the other; we can safely assume that the microstructure of the films used for the two measurements is the same. Hence, the results from the analyses of thermoelectric power and resistivity measurements can be combined.

From the plot of S_f against $1/t$, the intercept on the y axis gives S_g and the slope can be used to estimate U, the exponent in the energy-dependent mean-free-path expression, using the mean-free-path value evaluated from the conductivity data. The estimated Seebeck coefficient values of the infinite thick film S_g at 300, 350, and 400 K are -130, -132, and -133 $\mu V\,K^{-1}$. Using the mean free path calculated from the thickness-dependent resistivity data, the exponent U estimated has values 0.04, 0.05, and 0.07 at these temperatures. The values are very small, and hence the mean free path of the carriers is almost independent of energy.

Mayadas and Shatzkes[18] have shown that $1/\rho_g l_g=l/\rho_0 l_0$. From the free-electron theory, therefore,

$$1/\rho_0 l_0=\left[\frac{1}{3\pi^2}\right]^{1/3}\frac{e^2n^{2/3}}{\hbar}=1/\rho_g l_g\ ,$$

where n is the carrier concentration. Using the values of ρ_g and l_g the carrier concentration has been calculated at 300, 350, and 400 K. The values are found to be 1.10×10^{17}, 1.40×10^{17}, and 1.80×10^{17} carriers per cm^3.

The Fermi energy E_F has been evaluated from the Seebeck coefficient data using the expression for the Seebeck coefficient of the infinite thick film,

$$S_g=\frac{-\pi^2k^2T}{3eE_F}(1+U)\ .$$

Using the calculated carrier concentration and Fermi energy, the effective mass m^* of the carriers has been deter-

TABLE II. Comparison of the evaluated parameters with the published results.

Serial No.	Parameter	Temperature (K)	Present work	Published results
1	Electron concentration (cm^{-3})	300	1.1×10^{17}	9×10^{17} (at ~300 K)[a]
		350	1.4×10^{17}	2×10^{19}
		400	1.8×10^{17}	4.8×10^{18} (at 77 K bulk)[b]
2	Electron mean free path, l_g (Å)	300	5540	5960[c]
		350	4360	5540[c]
		400	3680	
3	Fermi energy (meV)	300	60	40[d]
		350	60	
		400	60	
4	Effective mass (m_e)	300	0.014	1.00
				0.32[e]
				0.105[d]
				0.101[a]
		350	0.017	
		400	0.020	
5	(Hypothetical) Bulk resistivity (ρ_g) (mΩ cm)	300	0.98	1.2 (ideal bulk)[b]
				2.0 (ideal bulk)[f]
		350	1.00	0.2–1.0 (ideal bulk)[g]
		400	1.00	(at ~300 K)
6	(Hypothetical) Bulk thermoelectric power, S_g (μV/K)	300	130	
		350	132	
		400	133	
7	Exponent U (see text)	300	0.04	
		350	0.05	
		400	0.07	

[a]Reference 27.
[b]Reference 15.
[c]Reference 8.
[d]Reference 28.
[e]Reference 29.
[f]Reference 22.
[g]Reference 13.

mined using the expression

$$E_F=\frac{\hbar^2}{2m^*}(3\pi^2 n)^{2/3}\ .$$

The various estimated parameters are tabulated in Table II and compared with those found in literature.

Since the carriers are partly degenerate, the effective mass of the carriers is much less than the values quoted in the literature. As the effective mass has been calculated in the present work using the above expression, its value depends directly on the carrier concentration n (as $\alpha n^{2/3}$) and inversely on the Fermi energy E_F. From Table II we find that our effective-mass values are of the same order as that reported earlier. However, our carrier concentration values are lower by a factor of 5 to 10 or more. Hence, the effective-mass values arrived at by us are also lower by a factor greater than 10. However, it is also evident that the carrier concentration values obtained by other earlier workers also differ by an order or more. Similarly, the effective-mass values obtained by other earlier workers also differ by an order (0.1 to 1.0). Apparently, the effective mass of the carriers depends on their concentration and degeneracy or otherwise. However, this is very speculative and much more work in that direction is needed before anything further can be said about the discrepancy.

CONCLUSIONS

The Seebeck coefficient and resistivity of Bi_2Te_3 thin films have been measured in the temperature range 300–470 K. The unannealed films show anomalous characteristics and irreversible behavior on heating. Therefore, the thermoelectric power and electrical conductivity data obtained only after annealing the films (at about 470 K for 1 h) have been used for the study of the size and temperature effects in Bi_2Te_3 thin films. The Seebeck coefficient and the resistivity of the annealed films have been found to be thickness and temperature dependent. The resistivity variation with temperature for annealed films shows good semiconducting behavior and $\ln\rho$ versus $1/T$ plots show a simple linear fit in the temperature range studied. The effective-mean-free-path model has been used to analyze the size effect of both the resistivity and the thermoelectric power of bismuth telluride thin films. The parameters such as the carrier concentration, the mean free path, and the effective mass have been determined. The estimated values have been compared with the quoted values in the literature.

[1]H. J. Goldsmid, J. Appl. Phys. **32**, 2198 (1969).
[2]C. H. Champness, W. B. Muir, and P. T. Chiang, Can. J. Phys. **45**, 3611 (1967).
[3]C. H. Champness, P. T. Chiang, and P. C. Parekh, Can. J. Phys. **43**, 653 (1965).
[4]C. H. Champness and A. L. Kipling, J. Phys. Chem. Solids **27**, 1409 (1966).
[5]C. H. Champness and A. L. Kipling, Can. J. Phys. **44**, 769 (1966).
[6]C. H. Champness, P. T. Chiang, K. Grabowaki, and W. B. Muir, J. Appl. Phys. **39**, 4177 (1968).
[7]C. H. Champness and P. C. Parekh, Can. J. Phys. **43**, 1589 (1965).
[8]A. Goswami and S. S. Koli, Indian J. Pure Appl. Phys. **7**, 166 (1969).
[9]B. M. Gol'tsman and M. G. Komissarchik, Fiz. Tverd. Tela (Leningrad) **15**, 301 (1973) [Sov. Phys.—Solid State **15**, 219 (1973)].
[10]M. J. McCulley, G. W. Neudeck, and G. L. Liedl, J. Vac. Sci. Technol. **10**, 391 (1973).
[11]M. H. Francombe, Philos. Mag. **10**, 989 (1964).
[12]P. S. Kireev, *Semiconductor Physics* (Mir Publishers, Moscow, 1978), p. 253.
[13]H. J. Goldsmid, Proc. Phys. Soc., London **71**, 633 (1958).
[14]R. Mansfield and W. William, Proc. Phys. Soc., London **72**, 733 (1958).
[15]J. R. Drabble, R. D. Grove, and R. Wolfe, Proc. Phys. Soc., London **71**, 430 (1958).
[16]H. J. Goldsmid, Proc. Phys. Soc., London **72**, 17 (1958).
[17]E. H. Sondheimer, Adv. Phys. (N.Y.) **1**, 1 (1952).
[18]A. F. Mayadas and M. Shatzkes, Phys. Rev. B **1**, 1382 (1970).
[19]E. E. Mola and J. M. Heras, Thin Solid Films **18**, 137 (1973).
[20]C. R. Tellier, A. J. Tosser, and C. Bontrit, Thin Solid Films **44**, 201 (1977).
[21]C. R. Tellier, Thin Solid Films **51**, 311 (1978).
[22]L. Ainsworth, Proc. Phys. Soc. Jpn. **11**, 915 (1956).
[23]H. Mayer, in *Structure and Properties of Thin Films*, edited by C. A. Neugebauer and J. B. Newkirk (Wiley, New York, 1959), p. 225.
[24]W. F. Leonard and S. F. Lin, J. Appl. Phys. **41**, 1868 (1970).
[25]P. Mikolajczak, W. Piasek, and M. Subotowcz, Phys. Status Solidi A **25**, 619 (1974).
[26]C. R. Pichard, C. R. Tellier, and A. J. Tosser, J. Phys. C **10**, 2009 (1980).
[27]R. B. Makkubsin, J. A. Rayne, and R. W. Ure, Jr., Phys. Rev. **175**, 1049 (1968).
[28]H. A. Ashworth, J. A. Rayne, and R. W. Ure, Jr., Phys. Rev. B **3**, 2646 (1971).
[29]T. C. Harman, S. E. Miller, and H. L. Goering, J. Phys. Chem. Solids **2**, 181 (1957).